IEEE Access
Multidisciplinary | Rapid Review | Open Access Journal

Received November 28, 2021, accepted December 26, 2021, date of publication February 3, 2022, date of current version February 11, 2022.

Digital Object Identifier 10.1109/ACCESS.2022.3146538

Close-Contact Detection Using a Single Camera for Sports Considering Occlusion

RYOSUKE HASEGAWA[1], AKIRA UCHIYAMA[1], (Member, IEEE), FUMIO OKURA[1], (Member, IEEE), DAIGO MURAMATSU[2], (Member, IEEE), ISSEI OGASAWARA[3], HIROMI TAKAHATA[3], KEN NAKATA[3], AND TERUO HIGASHINO[1], (Senior Member, IEEE)

[1]Graduate School of Information Science and Technology, Osaka University, Suita, Osaka 565-0871, Japan
[2]Faculty of Science and Technology, Seikei University, Musashino, Tokyo 180-8633, Japan
[3]Graduate School of Medicine, Osaka University, Suita, Osaka 565-0871, Japan

Corresponding author: Ryosuke Hasegawa (r-hasegawa@ist.osaka-u.ac.jp)

This work was supported by the Sports Research Innovation Project (SRIP) grant, sponsored by the Japan Sports Agency.

ABSTRACT The Coronavirus disease 2019 (COVID-19) is still prevalent in the world. Exercise is important to maintain our health while dealing with infectious diseases. Social distancing is more important during exercise because we may not be able to wear masks to avoid breathing problems, heatstroke, etc. To maintain social distancing during exercise, we develop a close-contact detection system using a single camera especially for sports in schools and gyms. We rely on a single camera because of the deployment cost. The system recognizes people from a video and estimates the interpersonal distance for close-contact detection. The challenge is the occlusion of people, which leads to false negatives in close-contact detection. To solve the problem, we leverage the observation that most false negatives in human detection are caused by occlusion owing to other people. This is because there are few obstacles in sports facilities. Based on the above observation, we assume that a person still exists near the last detected position even when s/he disappears in the proximity of other people. For evaluation, we recorded 834 videos that were 112 min long in total including various scenarios with 2724 close-contacts. The results show that the F1-score of close-contact detection and tracking are 83.6% and 67.3%, respectively. We also confirmed that the start and end time errors are within 1 s for more than 80% of the close-contacts.

INDEX TERMS Social distancing, COVID-19, human detection and tracking, distance estimation.

I. INTRODUCTION

The Coronavirus disease 2019 (COVID-19) is still prevalent in the world. Meanwhile, sports are important to maintain our health physically and mentally. Social distancing is more important during sports because we may not be able to wear masks to avoid breathing problems, heatstroke, etc [1]. Because vision-based human detection and tracking has been actively evaluated since before the pandemic, vision-based systems have been developed to support the management of social distancing [2]–[6]. These systems detect and track the skeletons or bounding boxes of humans to estimate interpersonal distance. However, the position error may increase during sports because the human pose changes frequently. Moreover, the tracking duration of close-contact is important in addition to distance among people because longer contact leads to higher risk [7]. For the supporting management of social distancing, the real-time warning of close-contacts is an effective way to avoid the risk of infection. It is also important to be able to analyze when and where the risk is high. This enables managers of sports facilities and teams to improve their behavior and rules.

To achieve the goal, we have developed a system designed for sports to detect and track close-contacts. Our system uses a single camera for low deployment costs and detects skeletons of people using *OpenPose* [8]. We select the waist position estimated by OpenPose to represent the position of the person for its stability in human detection. We then detect a close-contact when the distance between two persons becomes less than 2 m based on the definition of social distancing in Japan [9]. To improve the position error owing to the pose variation, we adjust the height of the waist according

The associate editor coordinating the review of this manuscript and approving it for publication was Kegen Yu.

to the pose of the legs. We proposed the basic concept of human localization with the waist height adjustment in Ref. [10]. In this work, we further propose the tracking of people and close-contacts based on the estimated positions of people. Specifically, for the tracking of close-contacts, the challenge is occlusion because we rely on a single camera. To solve the problem, we leverage the observation that most of the false negatives in human detection are caused by occlusion owing to other people. This is because there are few obstacles in sports facilities. Based on the above observation, we assume that a person still exists near the last detected position even when s/he disappeared in the proximity of other people.

To identify people at high risk of infection, it is necessary to identify the close-contact members. However, person identification [11]–[13] is another challenging topic which has been addressed by many researchers. Therefore, we exclude person identification (and inevitably human tracking) out of the scope of this paper. Instead, we focus on the tracking of close-contacts, i.e. measurement of close-contact duration regardless of involved persons. This is enough for the real time warning and the analysis of the time and locations with high risk to improve behavior and rules in sports facilities.

For evaluation, we recorded 834 videos that were 112 min in total including various scenarios with 2724 close-contacts. The results show that we achieve an F1-score of 83.6% for close-contact detection and an IDF1 [14] of 67.3% for close-contact tracking.[1] We also confirmed that the start and end times of more than 80% of the close-contacts are within 1 s, indicating that the close-contacts were correctly detected and tracked spatially and temporally. Additionally, we applied the system to an actual tennis tournament to support the management of social distancing. Through feedback on time and locations with frequent occurrences of close-contacts, we successfully suppressed the occurrence of close-contacts by changing the behavior of people.

Our contributions are summarized as below.

- We develop a close-contact detection and tracking system using a single camera for sports.
- To reduce the effect of pose variation on the position estimation, we adjust the position of the waist according to the pose of the legs.
- We design a close-contact tracking system, which is robust to occlusion based on the observation that occlusion in sport facilities is mostly caused by other people.
- To the best of our knowledge, this is the first study to evaluate the spatio-temporal correctness of close-contact detection and tracking.

II. RELATED WORK

A. LOCALIZATION

Localization is one of the key technologies for close-contact detection. Many researchers have proposed various methods using different types of devices such as radio frequency (RF) [15], light detection and ranging (LiDAR) [16], [17], and cameras [18]–[21]. Bluetooth and Wi-Fi are widely used for close-contact tracing owing to the wide availability of smartphones. However, the localization accuracy is typically up to a few meters [22], [23], which is not enough for distance-based close-contact detection. Recently, the millimeter wave has attracted the attention of researchers for localization because it has become available in IEEE 802.11ad and 5G cellular networks. Although it provides centimeter-level localization accuracy [15], the deployment cost is still large. Furthermore, because RF signals are reflected, refracted, and attenuated by people and walls, there are concerns about vulnerability to dynamic environment.

Using LiDAR, we can measure the distance to objects and humans with centimeter accuracy by measuring the time of flight of laser pulses. Refs. [16], [17] proposed target localization using LiDAR fixed in the target environment. However, we need to deploy LiDAR while incurring deployment cost although it can localize and track targets accurately.

Many camera-based localization methods have been proposed to detect humans using deep learning [18], [24], [25]. Some of them further detect humans with their skeletons [19], [20]. For the localization of a detected person, there are two major approaches: distance measurement using a stereo camera and homography using a single camera. For a stereo camera, we can measure the distance from the camera to a target by triangulation using the parallax between two cameras [21]. For a single camera, if we have four world points and their corresponding positions on the camera image plane, we can obtain the positions of any points on the same plane by homography transformation [26]. Because many people have camera devices including smartphones, a single camera-based approach has an advantage in terms of the deployment cost. Therefore, we design an approach based on a single camera in this study.

B. INFECTION PREVENTION

To avoid COVID-19 infection, researchers have already proposed several studies on monitoring interpersonal distance using a single camera [2]–[6]. Many of these studies use a person detector that outputs a bounding box containing a person. For example, D. Yang *et al.* [5] and P. Khandelwal *et al.* [4] calculated the inter-person distance using homography transformation with the bottom edge of the bounding box as the position of the person. However, the bottom edge of the bounding box does not always correspond to the same body part. For example, if a camera captures a whole body, the bottom edge of the bounding box corresponds to the foot position. However, if a camera captures only the upper body, the bottom edge of the bounding box corresponds to the waist position, leading to position error. Additionally, M. Rezaei *et al.* [2] and R. Keniya *et al.* [3] did not calculate the actual interpersonal distance but estimated whether each person violates social distance based on the size of the bounding box. However, the size of the bounding box varies

[1] IDF1 is the ratio of correctly identified detections over the average number of ground-truth and computed detections.

significantly depending on the pose. Therefore, we use a human skeleton detector and estimate the positions of humans based on their skeletons. Similarly, M. Aghaei *et al.* [6] used a skeleton detector for close-contact detection. However, they focused on the detection of close-contacts and did not consider the increase of the infection risk with time. Contrary to the previous work, we track close-contacts in addition to detection to measure their duration.

III. SYSTEM OVERVIEW

Figure 1 illustrates the overview of our system. Our target environment is sports activities in sports schools, gyms, etc. Our system consists of a single fixed camera and a computer for video processing. The camera is installed at a high place such as a ceiling to capture the target area in the angle of view. We detect and estimate the positions of humans in the captured image. We then calculate the interpersonal distance based on the estimated positions to detect the close-contact in real time. The system notifies a close-contact if detected. The system also records the positions and time of the detected close-contacts. By analyzing the records, managers of sports facilities and teams can find the time and places when and where close-contacts occur frequently for the improvement of their behavior and rules.

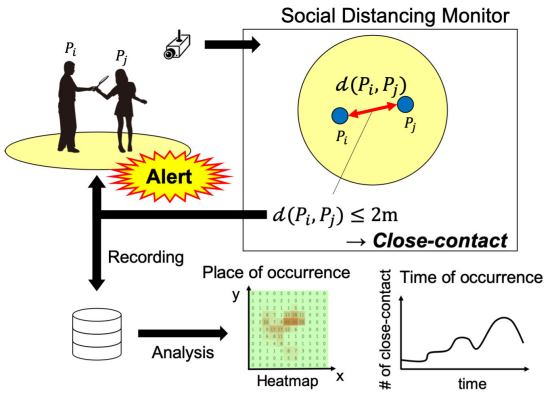

FIGURE 1. System overview.

IV. METHOD

A. OVERVIEW

Figure 2 shows the flow of our method. In each frame, we first detect persons using a state-of-the-art skeleton detector called *OpenPose-STAF* [8]. *OpenPose-STAF* detects and tracks a skeleton of a person in a video. Next, we estimate the position of the detected person based on the skeleton and the coordinates of four points whose positions are known. The four points correspond to the scene in the real world and we can transform coordinates of skeletons in an image into the actual positions. Finally, we detect a close-contact by calculating the interpersonal distance based on their positions. To mitigate the effect of occlusion, we track the detected people using *OpenPose-STAF*. We then assume that a person still exists near the last detected position even if s/he disappears in the proximity of other people. In this way, we avoid false negatives in the detection and tracking of close-contacts.

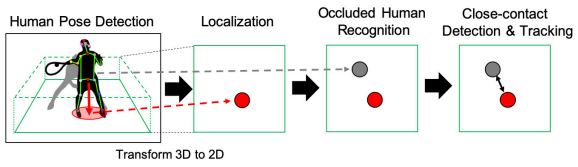

FIGURE 2. Method overview.

B. LOCALIZATION

1) HOMOGRAPHY TRANSFORMATION

For each frame, we estimate the position of the person whose skeleton is detected using *OpenPose-STAF*. For localization, we use the homography [26], which is a transformation that projects a plane to another plane, given the four point correspondences between the two planes. Therefore, a homography transformation matrix can transform pixel coordinates in an image into the actual positions, given the distance between the four points in the real world. This means that it is necessary to measure the distance between these four points in advance.

When a coordinate in an image is (u, v)[pixel], the corresponding coordinate (x, y)[m] in the real world is obtained by the following equation.

$$(x, y) = H(u, v) \tag{1}$$

H is the homography transformation matrix represented by the following equation.

$$H = \begin{bmatrix} h_{00} & h_{01} & h_{02} \\ h_{10} & h_{11} & h_{12} \\ h_{20} & h_{21} & 1 \end{bmatrix} \tag{2}$$

For each point with a given coordinate, we obtain two equations. Because H has eight variables, we can solve H, given the actual positions of the four points in the image.

Our method uses the key point of the waist for the reference key point whose position is regarded as the position of the person. This is because the waist key point is stably detected even during movement compared with other key points such as the legs.

We conducted a preliminary experiment to see how the height of each key point changes during movement. A subject moved across the front of a camera deployed at the height of 3m. We asked the subject to follow one of the three types of movements: walking, jogging, and running. The standard deviations of the key point heights for each movement type are shown in Table 1. From this result, we see that the waist height is more stable than the other key points. The height of the head fluctuated slightly less than the waist in walking and jogging. However, we see that the fluctuation becomes larger with the increase of movement intensity (i.e. running).

TABLE 1. Standard deviation of key points height during movement [cm].

Type \ Key Point	Waist	Head	Right Ankle	Left Ankle
Walking	3.32	2.94	11.89	5.88
Jogging	4.53	3.78	14.89	7.96
Running	4.51	8.55	37.54	24.26
Average	4.12	5.27	19.86	12.30

Therefore, the height of the four points for the homography transformation matrix is set to 0.9 m, which is the average waist height for adults.

2) WAIST HEIGHT CORRECTION

While walking and running, the height of the waist does not change significantly. However, it can change significantly depending on poses such as sitting on a chair or the ground. Because the height error leads to a position error after the transformation, we mitigate the effect by mapping the position of the waist onto the plane with the height of 0.9 m. The correction is performed before the homography transformation.

The overview of the correction is shown in Figure 3. We let a coordinate of key point k be $J^k = [u^k, v^k]$. The length $l(p, q)$ between key points p and q is defined as below.

$$l(p, q) = \sqrt{(u^p - u^q)^2 + (v^p - v^q)^2} \tag{3}$$

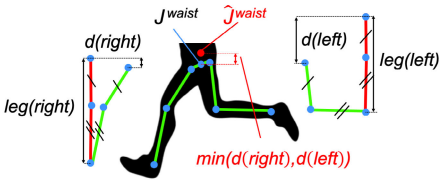

FIGURE 3. Waist height correction.

For each leg, *OpenPose-STAF* outputs three key points, which are the hip, knee, and ankle. The length $|leg|$ of the leg is obtained by combining the lengths between these joints as follows.

$$|leg| = l(hip, knee) + l(knee, ankle) \tag{4}$$

We refer to the difference between the ankle-to-hip height and $|leg|$ as the *correction distance* d. The correction distance is defined as below.

$$d = |leg| - (v^{hip} - v^{ankle}) \tag{5}$$

If the leg angle against the ground decreases, d increases. This means that the height of the reference key point (i.e. the waist) in the image is less than the assumed average waist height (i.e. 0.9 m). Therefore, we correct the hip height by adding d to the original hip height. However, there are some cases where the leg is not on the ground because of jumping, balancing, etc. For the waist height correction, we need to use d of the grounded leg because d is calculated assuming that the pose of the grounded leg lowers the waist height. If both legs are not on the ground, its duration is usually short. Therefore, we simply ignore such cases. However, when only one of the left and right legs is not on the ground, the vertical ankle-to-hip distance of the ungrounded leg becomes shorter than that of the grounded leg. In other words, d of the ungrounded leg is larger than the other because the lengths of the left and right legs should be almost the same. Therefore, we use either the left or right leg with the smaller correction distance. The coordinate of the waist $\hat{J}^{waist}$ after correction $\hat{v}^{waist}$ is given below.

$$\hat{v}^{waist} = v^{waist} + \min(d(left), d(right)) \tag{6}$$

We note that, if either of the legs is not detected, we do not perform the correction because we cannot determine whether the detected leg is on the ground.

C. HUMAN TRACKING

We use *Openpose-STAF* for human tracking. As mentioned earlier, occlusion is a major challenge in a single camera setting. We leverage the observation that most of the false negatives in human detection are caused by occlusion owing to other people in sports facilities. Therefore, we assume that a person still exists near the last detected position even when s/he disappeared in the proximity of other people.

Specifically, suppose ID^k is the set of IDs of humans detected in frame k. The IDs are given by *OpenPose-STAF*. For person i satisfying the following equation, the coordinate (x_i^{k-1}, y_i^{k-1}) in frame $k-1$ is defined as a *missing point*.

$$i \in ID^{k-1} \wedge i \notin ID^k \tag{7}$$

When a person is temporarily not detected because of occlusion, the corresponding missing point is defined. If we detect a person with a new ID within θ_d[m] from the missing point, we consider that the occlusion is resolved and delete the missing point. Meanwhile, a person may move during the occlusion, e.g. when multiple people are walking in a line. To deal with such cases, we delete a missing point if we do not detect any person with a new ID within θ_d[m] from the missing point for more than θ_ts. In this paper, we empirically set $\theta_d = 2.0$[m] and $\theta_t = 1/3$[sec].

D. CLOSE-CONTACT DETECTION AND TRACKING

We perform the close-contact detection and tracking based on the result of human tracking and estimated skeletons with the waist height correction. First, we calculate the distance between each pair of persons including the missing points. We denote the position of a person with ID i as P_i. We then calculate the distance $d(P_i, P_j)$ between persons i and j. If the following condition is satisfied, we detect a close-contact and define the midpoint between P_i and P_j as the point of the close-contact occurrence.

$$d(P_i, P_j) \leqq 2.0[\text{m}] \tag{8}$$

To obtain the duration and trajectory of the close-contact, we also track the close-contacts. For this purpose, it is

necessary to associate the close-contacts detected in the previous frame and those detected in the current frame. Because the close-contacts with a longer duration have a higher risk, we associate the close-contact with the longest duration in the previous frame with the nearest close-contact in the current frame within a distance θ_d. Our association algorithm is shown in Algorithm 1.

Algorithm 1 Tracking Close-contacts

Require: $C^p = \{c_1^p, c_2^p, \ldots, c_k^p\}(k \geq 0)$
$C^c = \{c_1^c, c_2^c, \ldots, c_n^c\}(n \geq 0)$

```
sort(C^p) // sort descending order of duration
for each c_i^p ∈ C^p do
    NearestID ← 0
    NearestDistance ← θ_d
    for each c_j^c ∈ C^c do
        if l(c_i^p, c_j^c) < NearestDistance then
            NearestID ← j
            NearestDistance ← l(c_i^p, c_j^c)
        end if
    end for
    if NearestID ≠ 0 then
        Associate(c_i^p, c^c_NearestID)
        sub (c^c_NearestID) from C^c
    end if
end for
```

V. EVALUATION

A. EVALUATION SETTING

We conducted four types of experiments to evaluate the performance of our system in terms of 1) the effect of waist height correction in localization, 2) the effect of human orientation in localization, 3) localization comparison with other methods, and 4) the accuracy of close-contact detection and tracking. The details of each experiment are as below.

1) EFFECT OF WAIST HEIGHT CORRECTION IN LOCALIZATION

For the evaluation of the effect of the waist height correction in the human localization, we collected images from one participant. We regard the position on the surface of the floor which is straight down from the waist as the actual position of the subject. Please note that we have not obtained the ground truth of the waist positions directly due to its difficulty. Instead, the subject located at one of the lattice points in Figure 4 with his waist straightly above the lattice points. He took five types of poses except one-leg-up as shown in Figure 5. The poses are standing, sitting (ground), sitting (chair), half-sitting, and crouching. For each pose (Figure 5) and location in the scenario (Figure 4), we obtained images in which all key points of the lower body were detected. For this purpose, we recorded videos of the subject facing the camera with the height of 2.5m. Finally, we collected 80 images.

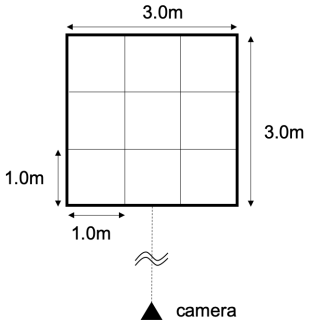

FIGURE 4. Evaluation area (Effect of waist height correction in localization).

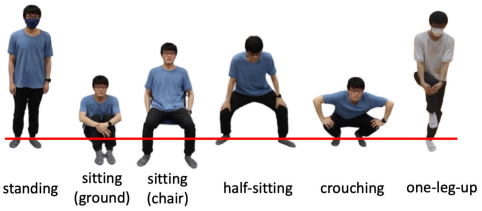

FIGURE 5. Poses used in evaluation.

2) EFFECT OF HUMAN ORIENTATION IN LOCALIZATION

For the evaluation of the robustness, we conducted evaluation in different camera positions and human orientations. One participant was located at one of the lattice points in Figure 6, and took six types of poses as shown in Figure 5. The poses are standing, sitting (ground), sitting (chair), half-sitting, crouching, and one-leg-up. There were two types of camera heights: 3.0m and 4.5m, and the participant faced four orientations: 0°, 90°, 180°, and 270°. The degree increases clockwise with 0° as the orientation when the person's body is facing the camera. Finally, we collected 2536 images.

3) LOCALIZATION COMPARISON WITH OTHER METHODS

Next, we compared our system with other methods using the same data as in Section V-A2. In many related works of close-contact detection, homography transformation is used for human localization. Therefore, we use other coordinates instead of the waist coordinates in homography transformation and compare the localization performance. We use the following two types of coordinates: the midpoint of the coordinates of both ankles [6], the bottom of the bounding box [2], [4], [5]. There is also a method for detecting close-contacts based on the size of the overlapping area of the bounding boxes [3]. However, since the distance between people is not calculated, we cannot compare our system with it. As the human detector that outputs bounding boxes, we used YOLOv4 [24] as in the Ref. [2] and [5].

4) CLOSE-CONTACT DETECTION AND TRACKING PERFORMANCE

For the evaluation of the close-contact detection and tracking performance, we collected data where the participants moved

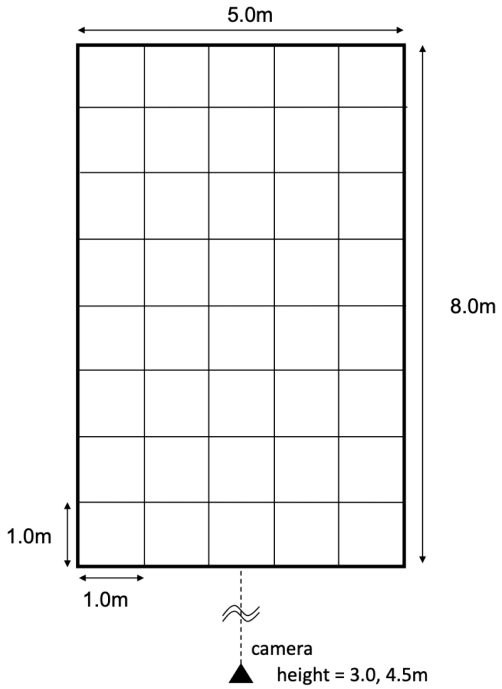

FIGURE 6. Evaluation area (Effect of human orientation in localization).

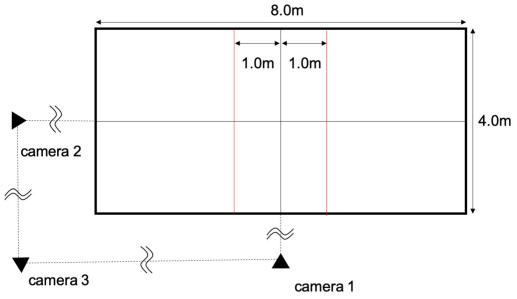

FIGURE 7. Evaluation area (Close-contact detection and tracking).

according to a predefined scenario. The participants moved in an area of 4.0 m × 8.0 m as shown in Figure 7. To determine the effect of the orientation of the person and the orientation of the occlusion, the images were taken from three different angles. To eliminate the effect of persons out of the target area, we pre-processed the images by manually specifying the target area.

There are three types of scenarios: (1) conversation, (2) passing each other, and (3) passing through. In all scenarios, each group consisting of one or two subjects moved according to the specified trajectories. In the case of two subjects, the distance between them was always kept within 2.0 m. The movement in each scenario is shown in Figure 8. In scenario (1), two groups walked from different starting positions toward the other group's starting position, stopped near the center, turned around, and walked back to their original positions. In scenario (2), two groups walked from

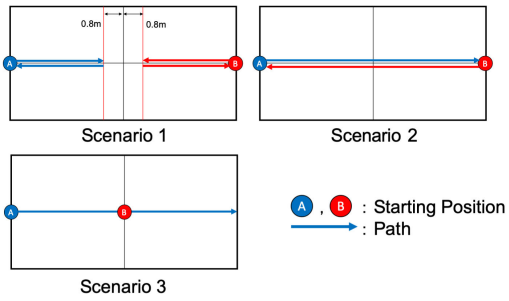

FIGURE 8. Movement scenarios.

different starting positions to the other group's starting position. In scenario (3), one group was stationary at a position, and the other group passed in front of or behind the other group. The stationary group was in one of three poses which are standing, sitting, and crouching. For each combination of a scenario, the number of subjects, and a pose, we recorded videos more than 10 times by randomly changing the subjects. Finally, we collected 278 videos. Because we used three cameras, the total number of videos was 834. Details of the data are listed in Tables 2 and 3.

TABLE 2. Details of data collection scenarios.

Scenario	Participants	Moves	Videos
1	1-1	10	30
	1-2	10	30
	2-2	10	30
2	1-1	10	30
	1-2	10	30
	2-2	10	30
3	(walking)1-1(stationary)	54	162
	1-2	54	162
	2-1	56	168
	2-2	54	162
Total	-	278	834

TABLE 3. Details of data collection in scenario (3).

Participants (Walking-Stationary)	Pose	Moves	Videos
1-1	standing	18	54
	sitting	18	54
	crouching	18	54
1-2	standing	18	54
	sitting	18	54
	crouching	18	54
2-1	standing	18	54
	sitting	20	60
	crouching	18	54
2-2	standing	18	54
	sitting	20	60
	crouching	16	48
Total	-	218	654

Each subject was asked to move at a constant speed on the trajectory specified in the scenario. However, the speed was slightly different for each participant and each trial.

Therefore, we recorded the start and end times of the movement as well as the time at the moment of crossing the red lines which are 1.0 m away from the center line as shown in Figure 7. The ground truth of the trajectories were then obtained by linear interpolation. We also obtained the ground truth of the close-contact occurrences from the ground truth of the trajectories.

B. RESULTS

1) EFFECT OF WAIST HEIGHT CORRECTION IN LOCALIZATION

First, we evaluated the localization performance. Table 4 lists the mean absolute error distance for each pose. From the results, we observe that we can estimate the position of the standing person with a low error. However, the error increases as the waist height gets closer to the ground. Additionally, we successfully decreased the error by an average of 23 cm.

TABLE 4. Mean absolute error for each pose [m].

Pose	Corrected	Original	Effect of correction
Standing	0.056	0.064	-0.008
Sitting (ground)	0.729	1.338	-0.609
Sitting (chair)	0.716	0.779	-0.063
Half-sitting	0.370	0.641	-0.271
Crouching	0.712	0.915	-0.203
Average	0.517	0.747	-0.231

However, we could not observe significant improvement for the pose of sitting on a chair. This is because the elevation angle of the camera and the angle of the leg were almost equal. When the relative angle of the leg (thigh and lower leg) to the camera is 0°, the leg length appears the shortest in the image while it appears the longest if the relative angle is 90°. In this experiment, the relative angle of the thigh to the camera was close to 0°, which means the appearance of the leg length in the image is shorter than the actual length.

To address this problem, we may need to obtain a more accurate leg length using a technique of estimating a 3D pose from a skeleton, for example.

2) EFFECT OF HUMAN ORIENTATION IN LOCALIZATION

Table 5 shows the localization performance for different body orientations and poses. As a result, when facing backwards (180°), the error was large in the poses such as sitting and crouching where the legs were hidden by the chair or the person's body itself because there were many false positives of the skeleton of the legs. In the standing pose, there are little difference of error in all orientations since there is no occlusion. This is due to the relationship between the camera and the legs as discussed in Section V-B1. Table 6 shows the localization error without the waist height correction. From this result, we see that the correction is effective in any orientation and pose. Even if the legs are bent, if they are facing to the side (90° or 270°), the whole lengths of the legs are visible in the image. Therefore, the performance greatly improves by the waist height correction.

TABLE 5. Mean absolute error [m] for different poses and orientations (with waist height correction).

Pose	Orientation			
	0°	90°	180°	270°
Standing	0.214	0.183	0.144	0.182
Sitting(ground)	1.867	0.819	2.523	0.491
Sitting(chair)	1.342	1.096	1.640	1.527
Half-sitting	0.474	0.589	0.553	0.648
Crouching	0.960	0.413	1.170	0.969
One-leg-up	0.316	0.287	0.200	0.310

TABLE 6. Mean absolute error [m] for different poses and orientations (w/o waist height correction).

Pose	Orientation			
	0°	90°	180°	270°
Standing	0.219	0.189	0.146	0.186
Sitting(ground)	1.990	2.240	2.247	2.292
Sitting(chair)	1.701	1.882	1.859	1.851
Half-sitting	0.743	0.885	1.002	0.894
Crouching	0.983	1.323	1.228	1.406
One-leg-up	0.313	0.217	0.188	0.248

3) LOCALIZATION COMPARISON WITH OTHER METHODS

Table 7 shows the localization error compared with the other methods. Since the data was collected in an unobstructed environment, the ground contact part of the body was visible without occlusion. Therefore, in poses such as sitting (chair) and half-sitting where the ankles are clearly visible, using the midpoint of the ankles shows the best result. The bottom of the bounding box showed the best results in poses such as sitting (ground) and crouching where the legs may be invisible depending on the orientation of the person. However, when using the midpoint of the ankles, the error increases significantly in a pose in which one leg is floating in the air. This is important because such a pose occurs frequently during exercise.

TABLE 7. Comparison of localization mean absolute error [m] with other methods.

Pose	Ours (waist)	Midpoint of ankles [6]	Bottom of box [2], [5]
Standing	**0.181**	0.211	0.286
Standing(0.3)	**0.244**	0.352	0.721
Standing(0.5)	**0.210**	0.333	1.344
Sitting(ground)	1.504	0.700	**0.515**
Sitting(chair)	1.475	**0.318**	0.393
Half-sitting	0.577	**0.211**	0.402
Crouching	0.931	**0.289**	0.436
One-leg-up	0.280	0.692	**0.230**

In addition, to evaluate the effect of occlusion, we virtually placed a wall at the feet by image processing when the participant takes a standing pose. The values in parentheses in Table 7 are the heights of the walls. In the method using the bottom of the bounding box, because the skeleton of the person is not estimated, it is not possible to determine whether the legs are hidden. The error thus increases significantly as the height of the virtual wall increases. In these cases, the increase of the error is mitigated by our method. However,

TABLE 8. Human detection result by scenarios.

# of participants	Scenario 1	2	3 standing	3 sitting	3 crouching
1-1	72.4	82.5	91.8	69.4	79.9
1-2	87.1	89.6	88.0	61.6	86.6
2-1			90.5	75.2	85.4
2-2	90.8	89.8	95.4	82.7	94.6

(a) Precision [%]

# of participants	Scenario 1	2	3 standing	3 sitting	3 crouching
1-1	98.6	99.0	94.9	81.7	94.3
1-2	97.4	98.5	96.6	70.7	97.3
2-1			97.6	85.2	96.6
2-2	96.9	95.4	95.4	84.5	96.1

(b) Recall [%]

TABLE 9. Close-contact detection result by scenarios.

# of participants	Scenario 1	2	3 standing	3 sitting	3 crouching
1-1	57.6	55.5	83.3	82.6	72.2
1-2	78.4	80.4	92.9	91.5	75.8
2-1	-	-	84.8	85.5	77.5
2-2	85.1	83.8	85.8	88.4	83.2

(a) Precision [%]

# of participants	Scenario 1	2	3 standing	3 sitting	3 crouching
1-1	89.0	88.9	93.3	90.9	77.7
1-2	85.7	87.3	92.9	90.6	72.8
2-1	-	-	90.5	88.9	82.1
2-2	86.9	86.2	81.0	78.1	73.9

(b) Recall [%]

our method has a larger error in sitting and crouching poses than the result in Section V-B1. This is due to false negatives of legs caused by the human detection. Especially, the pattern on the ground increased false positives in leg detection in a larger environment. This problem is due to the accuracy of the skeleton detector, which can be improved by properly using the detected skeletons depending on the situations. For example, we may use the waist key points when standing or moving, while we use the leg key points when sitting or stationary. Therefore, as future work, we leverage the poses of the person from the time-series data of the skeleton.

4) CLOSE-CONTACT DETECTION AND TRACKING PERFORMANCE

a: HUMAN DETECTION

For the evaluation of the human detection, we use precision and recall. For all results, the basic data to calculate precision, recall, and F1-score (i.e. the number of true positives, false positives, and false negatives) is shown in Table 13. If the distance between the ground truth and the estimated position is within 1.0 m, we regard the detection result as a true positive.

As a result, the precision and recall are 84.6% and 92.3%, respectively. The F1 score is 88.5%, indicating that many close-contacts are correctly detected spatially and temporally. The precision and recall for each scenario are listed in Table 8. From these results, we observe that there are almost no false negatives in any scenario. However, there are many false positives despite the scenarios with only two participants. This is because the marker lines on the floor were wrongly recognized as persons. In the scenarios with more people, the floor was hidden by them, leading to less false positives (i.e., increase of precision). To avoid the problem, we may consider the use of a high-resolution camera that can clearly capture the boundary between the floor and a person, or background subtraction to remove the effect of the floor pattern. In scenario 3, when there is a sitting participant, both precision and recall are lower than the other scenarios. This is because the waist height correction did not work well due to the wrong detection of legs. The skeleton detector wrongly recognized the chair as the legs of the person, leading to larger position error.

b: CLOSE-CONTACT DETECTION

For the evaluation of the close-contact detection, we use precision and recall. If the distance between the ground truth and estimated position is within 1.0 m, we regard the detection result as a true positive. As a result, the precision and recall are 83.9% and 83.4%, respectively. The F1 score is 83.6%, indicating that many close-contacts are correctly detected spatially and temporally. The precision and recall for each scenario are listed in Table 9. From these results, we observe that there are almost no false negatives in any scenario. Especially in the simple scenarios with a small number of people, we could detect close-contacts with higher recall.

However, there are many false positives in the simple scenarios. This is because there are many false positives in human detection in these scenarios. The precision of close-contact detection is lower than that of human detection. This happens when there are multiple people in close proximity. For example, if two true positives and one false positive are close to each other, the close-contact is detected between each pair. This means three close-contacts are detected. However, one of these is the correct close-contact while the other two are the wrong close-contacts. Therefore, in such a case, the number of false positives increases.

c: CLOSE-CONTACT TRACKING

Finally, we evaluated the close-contact tracking performance. We used the Identification Precision (IDP), Identification Recall (IDR) and Identification F1 (IDF1) proposed in Ref. [14] for the evaluation metrics to focus on the length of

TABLE 10. Close-contact tracking result by scenarios.

# of participants	Scenario 1	2	3 standing	3 sitting	3 crouching
1-1	54.8	**53.6**	**81.5**	**76.1**	**66.2**
1-2	**74.4**	**77.8**	**74.8**	**77.5**	58.9
2-1	-	-	**77.4**	**76.2**	**70.8**
2-2	**65.5**	**61.1**	**64.2**	**59.5**	**58.2**

(a) IDP [%]

# of participants	Scenario 1	2	3 standing	3 sitting	3 crouching
1-1	**84.5**	**85.8**	**91.3**	**83.8**	**71.3**
1-2	**81.3**	**84.5**	**74.8**	**76.7**	**56.5**
2-1	-	-	**82.6**	**79.2**	**75.0**
2-2	**66.9**	**62.8**	**60.6**	**52.6**	**51.7**

(b) IDR [%]

TABLE 11. Close-contact tracking result by scenarios w/o missing point.

# of participants	Scenario 1	2	3 standing	3 sitting	3 crouching
1-1	**56.4**	44.6	60.1	54.6	54.1
1-2	67.7	69.5	64.2	53.5	**62.3**
2-1	-	-	64.1	60.9	62.0
2-2	54.6	57.8	58.2	51.8	53.8

(a) IDP [%]

# of participants	Scenario 1	2	3 standing	3 sitting	3 crouching
1-1	62.1	62.4	50.1	41.6	42.4
1-2	67.1	68.0	57.6	40.0	54.4
2-1	-	-	60.2	54.1	56.2
2-2	46.6	53.2	48.0	35.6	41.3

(b) IDR [%]

correct tracking. This is reasonable because the duration of close-contacts is important for the assessment of the infection risk.

From the results, we confirmed that IDP, IDR, and IDF1 are 67.6%, 67.1%, and 67.3%, respectively. The precision and recall of each scenario are listed in Table 10. The IDP decreases in the scenario with a small number of subjects because of the false positives by the line markers on the floor as mentioned in Section V-B4.b. However, the IDR decreases with the increase of the number of subjects. This is because an ID frequently switched with another ID when multiple close-contacts occurred at the same time. One of the solutions to solve the problem is a Kalman filter for close-contact tracking to predict human and close-contact movement.

Next, Table 11 shows the precision and recall when occlusion is not considered (i.e. without the missing point). The best results in each scenario are shown in bold type. From these results, we have achieved significant performance improvements in many scenarios for both IDP and IDR by continuing to track hidden persons. Therefore, regardless of the frequency of occlusion, considering occlusions has a large effect. It is because the evaluation metrics IDP and IDR consider matching between close-contact IDs of the ground truth and the estimated result. For example, if ID switching occurs, all subsequent ground truth tracks and estimation tracks are considered as false negatives and false positives, respectively. Therefore, IDP and IDR become better if we keep the same close-contact IDs for each close-contact track for a longer time. This means that, regardless of the frequency of occlusion, even one occlusion may cause a large decrease in the tracking performance. Therefore, in many scenarios, the performance was improved by considering occlusion.

We also evaluated the start and end times of the close-contacts. Figure 9 shows the cumulative distribution function (CDF) of the absolute time error. The result shows that 85.1% of the start time error for all the close-contacts were within 30 frames (i.e., 1 s). 84.7% of the end time errors were also within 30 frames. Moreover, 71.0% of the elapsed time error were within 30 frames,whereas 86.0% of the elapsed time errors were within 60 frames (i.e., 2 s). This is reasonable because both of the start and end time errors are less than 1 s for more than 84.7% of the close-contacts. We also note that there is a little uncertainty in the ground truth of the subject positions (i.e., close-contact positions as well) owing to the manual labeling and linear interpolation.

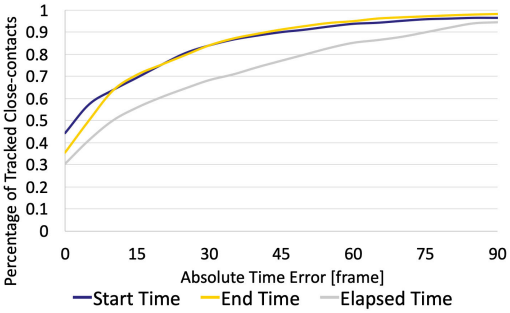

FIGURE 9. Time error in close-contact tracking.

TABLE 12. Close-contact occurrence during tennis tournament.

Day	Time	Close-contact over 4sec. Quantity	over 4sec. Frequency	All Quantity	All Frequency
1	5:39:41	184	32.5	806	142.4
2	6:17:45	208	33.0	940	149.2
3	1:51:18	29	15.6	147	79.2
3(Final)	1:23:42	34	24.4	158	113.3
All	15:12:26	455	29.9	2051	134.9

TABLE 13. The basic data to calculate precision, recall, and F1-score (True positives, false positives, false negatives).

# of participants	Scenario	Human Detection			Close-contact Detection			Close-contact Tracking			Close-contact Tracking w/o Missing Point		
		TP	FP	FN	TP	FP	FN	TP	FP	FN	TP	FP	FN
1-1	1	17179	6534	245	1831	1347	230	1740	1438	347	1279	989	787
	2	16638	3530	162	1747	1399	267	1686	1460	329	1226	1521	789
	3(standing)	25326	2265	1356	5280	1061	394	5168	1173	507	2837	1882	2822
	3(sitting)	21859	9641	4901	5309	1121	540	4895	1535	949	2477	2100	3449
	3(crouching)	25709	6486	1567	4393	1694	1245	4031	2056	1631	2352	1952	3329
1-2	1	25975	3832	692	11150	3069	2004	10586	3633	2634	8728	4164	4708
	2	22462	2603	335	9170	2234	1369	8876	2528	1680	7146	3129	3454
	3(standing)	36326	4940	1294	20755	1587	1824	16716	5626	5882	12867	7161	9659
	3(sitting)	25806	16082	10689	19616	1819	2023	16602	4833	5047	11769	7118	9713
	3(crouching)	35934	5579	1002	15704	5001	5652	12190	8515	9127	8578	7456	12864
2-1	3(standing)	36394	3839	902	19834	3554	2099	18099	5289	3860	13209	7383	8804
	3(sitting)	30403	10047	5291	20984	3565	2707	18707	5842	5062	13282	8131	10608
	3(crouching)	38739	6597	1356	17414	5070	3811	15909	6575	5340	11472	7367	9723
2-2	1	33610	3412	1058	22124	3876	3179	17027	8973	8182	11866	9872	13093
	2	29078	3312	1414	18005	3485	2814	13124	8366	7677	11117	8118	9669
	3(standing)	46789	2248	2231	34000	5636	8074	25442	14194	1658	20160	14493	21845
	3(sitting)	37961	7965	6967	36321	4768	29264	24449	16640	57671	19225	16500	77854
	3(crouching)	52650	3022	2118	28118	5679	9883	19665	14132	18475	13560	12593	24513

Nevertheless, our system could detect more than 80% of close-contacts with the start and end time errors within 0.83 s.

C. USE CASE

We used our system in a professional tennis tournament for safety management against COVID-19. We used close-contacts longer than 4 s in the following analysis because the normal interval between breaths is approximately 4 s. The results are listed in Table 12. In the table, the frequency refers to the number of close-contacts per hour. Because the number of staff (ball persons and line persons) was different in the final match on the third day, we analyzed the final match and other matches separately on the last day.

On the third day, the frequency of the close-contacts was lower than that of the first and second days. This is because we reported to the tournament management team on the situations (i.e., locations and timing) where close-contacts frequently occurred at the end of the second day. We noted that the frequency slightly increased in the final match owing to the increase of the number of staff. Overall, the frequency of the close-contacts decreased significantly after the report based on our system, highlighting its usefulness for safety management against COVID-19.

Additionally, we analyzed the time and locations of the close-contacts. First, the number of close-contacts over time is shown in Figure 10. Based on the analysis, we found that many close-contacts occurred not during the game but in between the games. Next, Figure 11 shows a heat map of the close-contact locations. From this result, we can observe that close-contacts occurred mostly in the center of the court and near the referee chair. As a result of checking the video, we found that players often moved around the referee chair at the changes of the ends and new balls were placed behind the referee chair, which is the cause of the frequent close-contacts. Additionally, some ball persons did not maintain a sufficient distance when they waited between games at the center of the court. Our system can support such analysis by providing spatial and temporal trends of close-contacts for safer risk management against COVID-19.

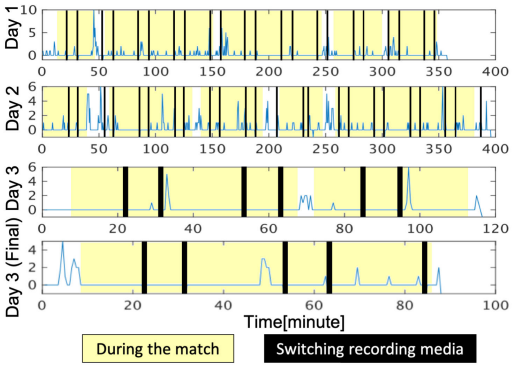

FIGURE 10. Time vs. Number of close-contacts.

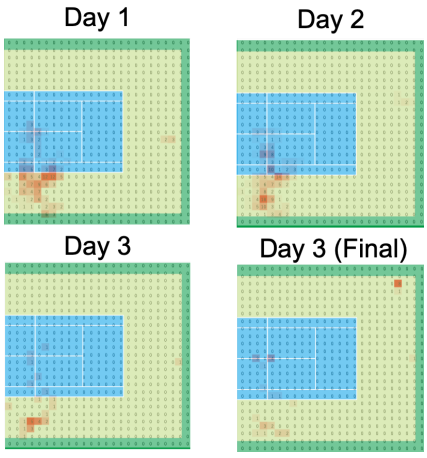

FIGURE 11. Place of occurrence.

VI. CONCLUSION

In this study, we proposed a close-contact detection and tracking system using a single camera during sports. We reduced the effect of the pose variation on the position estimation by adjusting the position of the detected person according to the pose of the legs. The evaluation results showed that our system achieved F1 scores of 83.6% and 67.3% for close-contact detection and tracking, respectively. Additionally, we confirmed that the start and end time errors were within 1 for more than 80% of the close-contacts.

One of our future works is to evaluate a method using the upper body skeleton for more robust position estimation. We also plan to deploy our system in various sports schools and gyms for our new lifestyle with COVID-19.

REFERENCES

[1] Ministry of Environment and Ministry of Health, Labor and Welfare in Japan. *Fiscal Year 2020 Heatstroke Prevention Actions*. Accessed: Oct. 21, 2021. [Online]. Available: https://www.otit.go.jp/files/user/docs/200615-5.pdf

[2] M. Rezaei and M. Azarmi, "DeepSOCIAL: Social distancing monitoring and infection risk assessment in COVID-19 pandemic," *Appl. Sci.*, vol. 10, no. 21, p. 7514, 2020.

[3] R. Keniya and N. Mehendale, "Real-time social distancing detector using socialdistancingnet-19 deep learning network," *SSRN Preprint*, Aug. 2020.

[4] P. Khandelwal, A. Khandelwal, S. Agarwal, D. Thomas, N. Xavier, and A. Raghuraman, "Using computer vision to enhance safety of workforce in manufacturing in a post COVID world," 2020, *arXiv:2005.05287*.

[5] D. Yang, E. Yurtsever, V. Renganathan, K. A. Redmill, and Ü. Özgüner, "A vision-based social distancing and critical density detection system for COVID-19," 2020, *arXiv:2007.03578*.

[6] M. Aghaei, M. Bustreo, Y. Wang, G. Bailo, P. Morerio, and A. D. Bue, "Single image human proxemics estimation for visual social distancing," in *Proc. IEEE Winter Conf. Appl. Comput. Vis. (WACV)*, Jan. 2021, pp. 2785–2795.

[7] V. Vlacha, G. Feketea, A. Petropoulou, and S. D. Trancá, "The significance of duration of exposure and circulation of fresh air in SARS-CoV-2 transmission among healthcare workers," *Frontiers Med.*, vol. 8, Jun. 2021, Art. no. 664297.

[8] Y. Raaj, H. Idrees, G. Hidalgo, and Y. Sheikh, "Efficient online multi-person 2D pose tracking with recurrent spatio-temporal affinity fields," in *Proc. IEEE/CVF Conf. Comput. Vis. Pattern Recognit. (CVPR)*, Jun. 2019, pp. 4620–4628.

[9] Ministry of Environment and Ministry of Health, Labor and Welfare in Japan. *Example of Practicing New Lifestyle*. Accessed: Oct. 21, 2021. [Online]. Available: https://www.mhlw.go.jp/content/10900000/000632485.pdf

[10] R. Hasegawa, A. Uchiyama, F. Okura, D. Muramatsu, I. Ogasawara, H. Takahata, K. Nakata, and T. Higashino, "Human localization using a single camera towards social distance monitoring during sports," in *Proc. EAI Int. Conf. Mobile Ubiquitous Syst.*, 2021.

[11] M. Ye, J. Shen, G. Lin, T. Xiang, L. Shao, and S. C. H. Hoi, "Deep learning for person re-identification: A survey and outlook," *IEEE Trans. Pattern Anal. Mach. Intell.*, early access, Jan. 26, 2021, doi: 10.1109/TPAMI.2021.3054775.

[12] D. Fu, D. Chen, J. Bao, H. Yang, L. Yuan, L. Zhang, H. Li, and D. Chen, "Unsupervised pre-training for person re-identification," in *Proc. IEEE/CVF Conf. Comput. Vis. Pattern Recognit. (CVPR)*, Jun. 2021, pp. 14750–14759.

[13] G. Wang, J. Lai, P. Huang, and X. Xie, "Spatial-temporal person re-identification," in *Proc. AAAI Conf. Artif. Intell.*, vol. 33, 2019, pp. 8933–8940.

[14] E. Ristani, F. Solera, R. Zou, R. Cucchiara, and C. Tomasi, "Performance measures and a data set for multi-target, multi-camera tracking," in *Proc. Eur. Conf. Comput. Vis.* Cham, Switzerland: Springer, 2016, pp. 17–35.

[15] C. Wu, F. Zhang, B. Wang, and K. J. Ray Liu, "MmTrack: Passive multi-person localization using commodity millimeter wave radio," in *Proc. IEEE INFOCOM Conf. Comput. Commun.*, Jul. 2020, pp. 2400–2409.

[16] M. Hasan, J. Hanawa, R. Goto, H. Fukuda, Y. Kuno, and Y. Kobayashi, "Tracking people using ankle-level 2D LiDAR for gait analysis," in *Proc. Int. Conf. Appl. Hum. Factors Ergonom.* Cham, Switzerland: Springer, 2020, pp. 40–46.

[17] Y.-T. Wang, C.-C. Peng, A. A. Ravankar, and A. Ravankar, "A single LiDAR-based feature fusion indoor localization algorithm," *Sensors*, vol. 18, no. 4, p. 1294, Apr. 2018.

[18] S. Bahadori, L. Iocchi, G. R. Leone, D. Nardi, and L. Scozzafava, "Real-time people localization and tracking through fixed stereo vision," *Int. J. Speech Technol.*, vol. 26, no. 2, pp. 83–97, Mar. 2007.

[19] J. Lin and G. H. Lee, "HDNet: Human depth estimation for multi-person camera-space localization," in *Proc. Eur. Conf. Comput. Vis.* Cham, Switzerland: Springer, 2020, pp. 633–648.

[20] W. Zhang, Z. Liu, L. Zhou, H. Leung, and A. B. Chan, "Martial arts, dancing and sports dataset: A challenging stereo and multi-view dataset for 3D human pose estimation," *Image Vis. Comput.*, vol. 61, pp. 22–39, May 2017.

[21] M. Kytö, M. Nuutinen, and P. Oittinen, "Method for measuring stereo camera depth accuracy based on stereoscopic vision," *Proc. SPIE*, vol. 7864, Jan. 2011, Art. no. 78640I.

[22] R. Zhou, M. Hao, X. Lu, M. Tang, and Y. Fu, "Device-free localization based on CSI fingerprints and deep neural networks," in *Proc. 15th Annu. IEEE Int. Conf. Sens., Commun., Netw. (SECON)*, Jun. 2018, pp. 1–9.

[23] M. Abbas, M. Elhamshary, H. Rizk, M. Torki, and M. Youssef, "WiDeep: WiFi-based accurate and robust indoor localization system using deep learning," in *Proc. IEEE Int. Conf. Pervasive Comput. Commun. (PerCom*, Mar. 2019, pp. 1–10.

[24] A. Bochkovskiy, C.-Y. Wang, and H.-Y. M. Liao, "YOLOv4: Optimal speed and accuracy of object detection," 2020, *arXiv:2004.10934*.

[25] S. Ren, K. He, R. Girshick, and J. Sun, "Faster R-CNN: Towards real-time object detection with region proposal networks," *IEEE Trans. Pattern Anal. Mach. Intell.*, vol. 39, no. 6, pp. 1137–1149, Jun. 2017.

[26] D. Capel and A. Zisserman, "Computer vision applied to super resolution," *IEEE Signal Process. Mag.*, vol. 20, no. 3, pp. 75–86, May 2003.

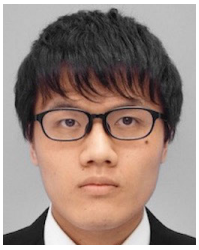

RYOSUKE HASEGAWA received the M.E. degree in information and computer science from Osaka University, Japan, in 2019, where he is currently pursuing the Ph.D. degree with the Graduate School of Information Science and Technology. His current research interests include sensing and data analytics for sports. He is a member of the Information Processing Society of Japan (IPSJ).

AKIRA UCHIYAMA (Member, IEEE) received the M.E. and Ph.D. degrees in information and computer science from Osaka University, in 2005 and 2008, respectively. From 2007 to 2009, he was a Research Fellow with the Japan Society for the Promotion of Science. He was a Visiting Scholar with the University of Illinois at Urbana–Champaign, in 2008. He is currently an Associate Professor with the Graduate School of Information Science and Technology, Osaka University. His current research interests include mobile sensing and applications in pervasive and ubiquitous computing. He is a member of ACM, IEICE, and IPSJ.

FUMIO OKURA (Member, IEEE) received the M.S. and Ph.D. degrees in engineering from the Nara Institute of Science and Technology, in 2011 and 2014, respectively. He was an Assistant Professor with the Institute of Scientific and Industrial Research, Osaka University, until 2020. He is currently an Associate Professor with the Graduate School of Information Science and Technology, Osaka University. His research interest includes boundary domain between computer vision and computer graphics.

DAIGO MURAMATSU (Member, IEEE) received the B.S., M.E., and Ph.D. degrees in engineering from Waseda University, Tokyo, Japan, in 1997, 1999, and 2006, respectively. From 2015 to 2020, he was an Associate Professor with the Institute of Scientific and Industrial Research, Osaka University. He is currently a Professor with the Department of Computer and Information Science, Faculty of Science and Technology, Seikei University. His research interests include pattern recognition, and biometrics including gait recognition. He is a member of IPSJ and IEICE.

ISSEI OGASAWARA received the M.S. degree in sports sciences and the Ph.D. degree in sports medicine from the University of Tsukuba, in 2005 and 2009, respectively. He worked at the National Institute of Advanced Industrial Science and Technology, in 2005, and the Japan Institute of Sports Sciences, from 2006 to 2011. He is currently an Assistant Professor with the Graduate School of Medicine, Osaka University. He is also conducting several research projects, including preventing and predicting severe athletic injuries, bio-mechanical assessment of movement disorder, and evaluating physical intensity in a real-world sports environment.

HIROMI TAKAHATA majored in communication engineering at the Nara Institute of Science and Technology until 2008. She majored in medical and biological engineering at the Graduate School of Engineering, Osaka University, and received the Ph.D. degree in 2014. In 2013, she joined the National University of Singapore as a Research Fellow. Since 2015, she has been an Assistant Professor with the Graduate School of Medicine, Osaka University, conducting research in the field of sports medicine to prevent injuries and improve athletes' competitiveness using sensor devices and images.

KEN NAKATA received the M.D. and Ph.D. degrees from Osaka University, Japan, in 1986 and 1993, respectively. In 1993, he joined the National Institutes of Health as a Postdoctoral Fellow. From 1996 to 1999, he was an Assistant Professor with the Department of Orthopaedic Surgery, Osaka University Graduate School of Medicine. From 2000 to 2003, he was the Chief of sports orthopaedic surgery at Kansai Rosai Hospital, and became an Associate Professor with the Department of Orthopaedic Surgery, Osaka University Graduate School of Medicine, in 2003. He has been a Professor and the Chairperson of Medicine for Sports and Performing Arts, Department of Health and Sport Sciences, Osaka University Graduate School of Medicine, since 2013. His current research interests include sports medicine, biomechanics, and molecular mechano-biology. He is the President of Japanese Clinical Biomechanics, the Director of the Japanese Society of Cartilage Metabolism and the International Clinical Medicine, and a member of the Japan Orthopaedic Association.

TERUO HIGASHINO (Senior Member, IEEE) received the B.S., M.S., and Ph.D. degrees in information and computer sciences from Osaka University, Japan, in 1979, 1981, and 1984, respectively. In 1984, he joined Osaka University as a Faculty Member. From 2002 to 2021, he was a Professor with the Graduate School of Information Science and Technology, Osaka University. He has been a Specially Appointed Professor with Osaka University and a Professor with Kyoto Tachibana University, since 2021. His current research interests include design and analysis of distributed systems, communication protocol, and mobile computing. He is a member of ACM and IEICE of Japan and a fellow of the Information Processing Society of Japan (IPSJ).